AD-A192 307 ATOMIC LAYER EPITAXY OF ZNS AND ZNSE(U) ROCKWELL INTERNATIONAL THOUSAND OAKS CA SCIENCE CENTER J G NELSON FEB 88 SC5461.FR ARMSEL-NV-1-21 1/1

UNCLASSIFIED DAAB07-86-C-F013 F/G 7/2 NL

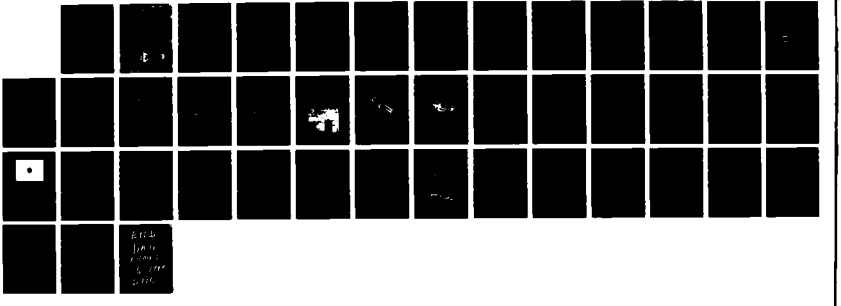

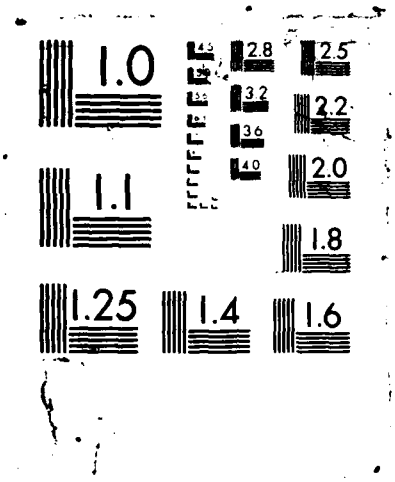
1.0
2.8
2.5
3.2
2.2
3.6
4.0
2.0
1.1
1.8
1.25
1.4
1.6

Center for Night Vision and Electro-Optics

CONTRACT NUMBER

DAAB07-86-C-F013

REPORT NUMBER

SC5461.FR

Atomic Layer Epitaxy of ZnS and ZnSe

J.G. Nelson

Rockwell International Science Center
1049 Camino Dos Rios
Thousand Oaks, CA 91360

Final Report

February 1988

FORT BELVOIR, VA 22060-5677

UNCLASSIFIED

SECURITY CLASSIFICATION OF THIS PAGE

REPORT DOCUMENTATION PAGE

FORM APPROVED OMB No. 0704-0188

1a. REPORT SECURITY CLASSIFICATION
UNCLASSIFIED

1b. RESTRICTIVE MARKINGS
None

2a. SECURITY CLASSIFICATION AUTHORITY
N/A

2b. CLASSIFICATION/DOWNGRADING SCHEDULE
N/A

3. DISTRIBUTION/AVAILABILITY OF REPORT
Approved for public release; distribution unlimited

4. PERFORMING ORGANIZATION REPORT NUMBER(S)
SC5461.FR

5. MONITORING ORGANIZATION REPORT NUMBER(S)
NV-1-21

6a. NAME OF PERFORMING ORGANIZATION
ROCKWELL INTERNATIONAL Science Center

6b. OFFICE SYMBOL (If Applicable)

7a. NAME OF MONITORING ORGANIZATION
Center for Night Vision & Electro-Optics

6c. ADDRESS (City, State, and ZIP Code)
1049 Camino Dos Rios Thousand Oaks, CA 91360

7b. ADDRESS (City, State and ZIP Code)
Ft. Belvoir, VA 22060-5677

8a. NAME OF FUNDING/SPONSORING ORGANIZATION
Center for Night Vision & Electro-Optics

8b. OFFICE SYMBOL (If Applicable)
AMSEL-RD-NV-L

9. PROCUREMENT INSTRUMENT IDENTIFICATION NUMBER
CONTRACT NO. DAAB07-86-C-F013

8c. ADDRESS (City, State and ZIP Code)
Laser Division Ft. Belvoir, VA 22060-5677

10. SOURCE OF FUNDING NOS.

PROGRAM ELEMENT NO	PROJECT NO.	TASK NO.	WORK UNIT ACCESSION NO.
62709A	IL162709 DH95	8.0	001/DA31 0617

11. TITLE (Include Security Classification)
ATOMIC LAYER EPITAXY OF ZnS AND ZnSe

12. PERSONAL AUTHOR(S)
Nelson, J.G.

13a. TYPE OF REPORT	13b. TIME COVERED	14. DATE OF REPORT (Year, Month, Day)	15. PAGE COUNT
Final Report	FROM 05/08/86 TO 06/18/87	1988, FEBRUARY	40

16 SUPPLEMENTARY NOTATION
"The views, opinions, and/or findings in this report are those of the author(s) and should not be construed as an official Department of the Army position, policy or decision, unless designated by other documentation."

17 COSATI CODES		
FIELD	GROUP	SUB-GROUP
20	12	5

18. SUBJECT TERMS (Continue on reverse if necessary and identify by block number)
Atomic layer epitaxy, ZnSe, ZnTe, IR rugate

19 ABSTRACT (Continue on reverse if necessary and identify by block number)

The objective of this program was to determine the feasibility of using Atomic Layer Epitaxy (ALE) as a deposition technique for fabricating IR rugate structures. Theoretical activities under the contract consisted of designing and modeling rugate structures containing ZnS and ZnSe or ZnSe and ZnTe. The experimental work resulted in the growth of high-quality epitaxial films of ZnS, ZnSe and ZnTe on (001)-oriented GaAs substrates. Multi-layer structures (quarter-wave stacks and rugate filters) of ZnSe and ZnTe were deposited; but although certain aspects of these ALE structures were successful, the devices did not show the optical performance that was expected. This has been understood as resulting from differences in film nucleation and growth rates between the two candidate materials which were chosen for this program.

Our conclusions are that, although ALE is capable of producing high-quality epitaxial and chalcogenide thin films, it is not a practical technique for fabricating IR rugate filters.

20 DISTRIBUTION/AVAILABILITY OF ABSTRACT
UNCLASSIFIED/UNLIMITED ☐ SAME AS RPT. ☒ DTIC USERS ☐

21 ABSTRACT SECURITY CLASSIFICATION
UNCLASSIFIED

22a NAME OF RESPONSIBLE INDIVIDUAL
Byong H. Ahn

22b. TELEPHONE NUMBER (Include Area Code)
(703) 664-5364

22c OFFICE SYMBOL
AMSEL-RD-NV-L

DD FORM 1473, JUN 86 **Previous editions are obsolete.**

UNCLASSIFIED

SECURITY CLASSIFICATION OF THIS PAGE

SC5461.FR

Copy No._____

ATOMIC LAYER EPITAXY OF ZnS AND ZnSe

FINAL REPORT FOR THE PERIOD May 30, 1986 through June 18, 1987

CONTRACT NO. DAAB07-86-C-F013

Prepared for

Center for Night Vision and Electro-Optics
Laser Vision
Ft. Belvoir, VA 22060-5677

Attn: Byong H. Ahn, Code W26P71

J.G. Nelson
Principal Investigator

FEBRUARY 1988

TABLE OF CONTENTS

LIST OF FIGURES

LIST OF FIGURES

LIST OF FIGURES

LIST OF FIGURES

PREFACE

This report describes research conducted by Rockwell International Science Center for the Center for Night Vision & Electro-Optics, Fort Belvoir, VA. The work was performed under Contract No. DAAB07-86-C-F013.

The work reported herein was performed during the period May 8, 1986 through June 18, 1987. The report was submitted by the author in October 1987.

The author would like to thank Mr. Byong Ahn of CNVEO for his direction and support during the research.

SUMMARY

Rugate filters are a specific class of gradient-index optical thin-film structures. Reflection of a single wavelength band is accomplished by interference caused by a sinusoidal modulation of the refractive index of the structure. The width of the reflectance band is proportional to the index modulation and the reflectance amplitude is proportional to the number of periods, or filter thickness.

Atomic Layer Epitaxy (ALE) is a physical vapor deposition technique which permits a high degree of thickness control and the perfection of single crystal epitaxial thin films which have bulk-like optical and physical properties. This technique was investigated as a method of fabricating rugate filters because it is able to address issues such as film thickness control, film uniformity and device compatibility with high-power optics, which are important in this type of device. Bulk-like thin-film properties improve the device effectiveness in high-power optics, while film thickness control and film uniformity are essential to accurately and reproducibly fabricate the filter.

In this report, we describe the results of a one-year program to investigate the feasibility of using ALE to fabricate IR rugate filters. The goals of this program were to increase the deposition rate of ALE, to determine the optimum growth parameters needed to deposit high-quality epitaxial films of ZnS, ZnSe and ZnTe and to apply these results to the fabrication of rugate structures by ALE.

Early studies using thermal evaporation of S, Se and Zn to produce ZnS and ZnSe films showed that high-quality single-crystal epilayers of these compounds could be grown on GaAs substrates. Optimum growth parameters such as substrate temperature, source crucible temperature and growth cycle time were determined for the two systems.

In an attempt to increase the deposition rate of ALE in addition to improving source material utilization, experiments were performed using a Nd:YAG laser to evaporate elemental materials instead of thermal evaporation. S was found unsuitable for laser deposition so ZnS was replaced by the similar compound ZnTe as the second material to be used in the rugate structure. Additional studies using thermal evaporation of Zn and Te were performed to completely characterize the growth parameters for the two materials which would be used in the optical films.

Multilayer structures of ZnSe and ZnTe were deposited to assess the agreement between the measured and predicted performance of these simple optical structures. Several rugate filter fabrication runs were made where the number of sinusoidal periods varied from 3 to 8. Although certain aspects of these ALE structures were successful, the devices did not show the optical performance that was expected.

Based on the results of this study, we conclude that, although ALE is capable of producing high-quality epitaxial films of the zinc chalcogenides, it is not a suitable technique for fabricating thick IR rugate structures. It appears that the growth kinetics of the ALE process will limit the growth rate to less than 2 Å/s. This rate is simply too slow to be of practical use for fabricating a structure which is in excess of ~ 20 μm in total thickness.

1.0 INTRODUCTION

1.1 Rugate Filters

Rugate filters are a specific class of gradient-index optical thin-film structures. These filters employ a sinusoidal index profile to achieve spectral interference effects, as opposed to standard optical multilayers which use the Fresnel reflection from discrete layer interfaces to provide a means for the interference phenomena. Rugates reflect a single wavelength band without the shorter wavelength harmonics observed in conventional quarter-wave stack filters. As with quarter-wave stack filters, the reflective bandwidth is proportional to the peak-to-peak refractive index modulation, N_p, and the peak reflectance is proportional to the N_p times the number of periodic cycles.

One approach to fabricating rugate structures is to make use of the fact that smoothly varying index media may be approximated by discrete layers of infinitesimal thickness. Although infinitesimally thin layers are not possible, a practical limit of $\lambda/(80\ n)$ is useful in determining the maximum thickness of each individual layer. This so-called "digital" concept was used in designing and modeling the rugate structures under this program.

ALE was chosen as a possible technique for fabricating advanced optical structures such as rugate filters because it has several advantages over other deposition methods. Under ideal conditions, thin films are deposited a single atomic layer at a time, allowing precise thickness control which is necessary for multilayer rugate fabrication. Film uniformity is on the same scale as the thickness control. Since films deposited by ALE exhibit bulk optical and physical properties, these optical thin films are compatible with high-power laser optics which tend to degrade or destroy structures which contain defects associated with less than bulk-like thin films.

Currently ALE is used for growing epitaxial or highly-oriented thin films of either III-V or II-VI compound semiconductors.[1-11] To insure complete and accurate layer by layer growth, most workers use long cycle times which correspond to growth rates of between 0.067 and 0.12 Å/s. To date, no studies have been performed to calculate a theoretical maximum for the ALE growth kinetics of these systems. Therefore, it is not clear whether the ultimate growth rate will be determined by the growth kinetics or by mechanical considerations such as system pumping speed, source to substrate distance and background pressure during the film deposition.

1.2 ALE Process

The II-VI compound semiconductors have considerable potential for optoelectronic device applications. Atomic Layer Epitaxy (ALE) has been demonstrated to be an excellent technique for growing such II-VI films.[1-3] ALE was first described in a U.S. Patent of Finnish origin filed in 1975,[4] which describes a method for producing compound thin films such as ZnS, SnO_2, and GaP. The initial work was continued by Pessa's group at the University of Tampere in Finland. They described various aspects of the technique, in particular surface analysis studies of the reactions occurring on the substrate[5,6] and investigations into the crystal structure of the resulting films.[7-9]. Pessa's work concentrated largely on ZnS and CdTe. ALE growth of ZnSe and ZnTe was first reported by Yao[2] in 1986. The first reports on the growth of III-V compound semiconductors by ALE came from Bedair[10] in U.S. and Nishizawa[11] in Japan.

A thin film of a compound material is grown by ALE by depositing alternating layers of the constituent elements. At time zero, the first component beam impinges on the substrate. The flux of the material should be sufficient to form slightly more than one complete layer. If the substrate temperature is sufficiently high, only one monolayer of the element will adhere to the surface, while the rest of the material re-evaporates. This single monolayer sticks to the surface because the compound bond formed by the monolayer to the existing surface layer is stronger than the elemental bond formed between the individual atoms of that particular element. This is illustrated in Figs. 1.1 and 1.2 which show the re-evaporation rate of the thin-film compounds compared to that of the constituent elements. After a short time interval, during which the as-grown film is self-adjusting its stoichiometry, structure and thickness (i.e., reaching equilibrium), the first atomic beam is terminated and the second elemental beam is turned on. Once again, more than one monolayer of the second element initially condenses on the substrate surface, but due to the increased strength of the compound bond (II-VI) with respect to an elemental bond (II-II or VI-VI), all but a single monolayer of the element will re-evaporate. This process is shown schematically in Fig. 1.3. In part (a), the atoms of one particular element strike the substrate surface and adhere. In (b), one complete monolayer has finally formed. After the completion of one elemental monolayer, the rest of the atoms in the beam do not stick to the surface (part c). Next, the same sequence of events occurs using the second elemental material. This entire process is repeated until the desired film thickness is achieved. Due to the controlled nature of this deposition technique, the incremental thickness gain for each atomic layer is simply the interplanar spacing in the growth direction.

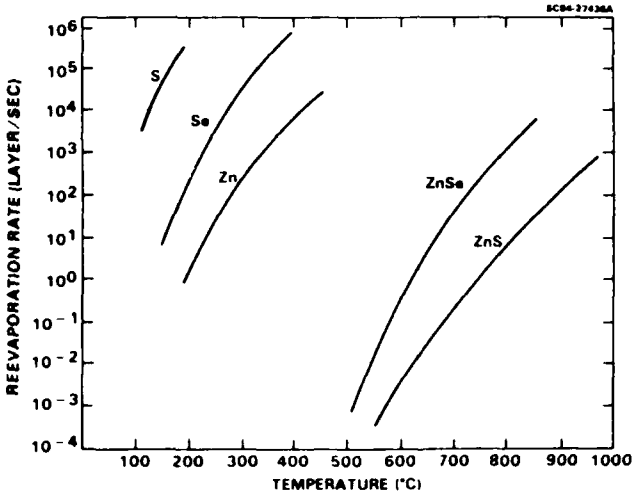

Fig. 1.1 Re-evaporation rate as a function of temperature for elemental Zn, S and Se and for the compounds ZnS and ZnSe.

A useful approach to understanding the growth mechanism of ALE is to consider the difference between chemisorption and physisorption of atoms on the substrate surface. In chemisorption, strong forces occur when chemical bonds are formed with a substrate and the heat of adsorption (ΔH_{ads}) is negative; i.e., the adsorption of gases and vapors on solids is an exothermic reaction. Because chemisorption involves the formation of surface bonds and physisorption is only a van der Waals type of interaction, the heats of chemisorption are about one order of magnitude larger than the heats of physisorption.

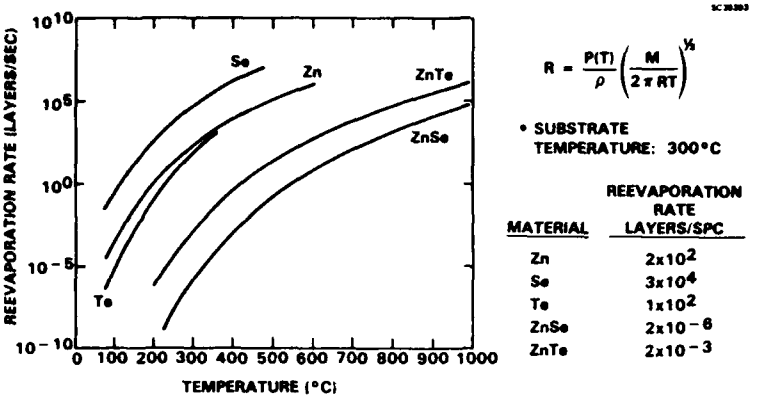

Fig. 1.2 Re-evaporation rate as a function of temperature for elemental Zn, Se, Te and for the compounds ZnSe and ZnTe.

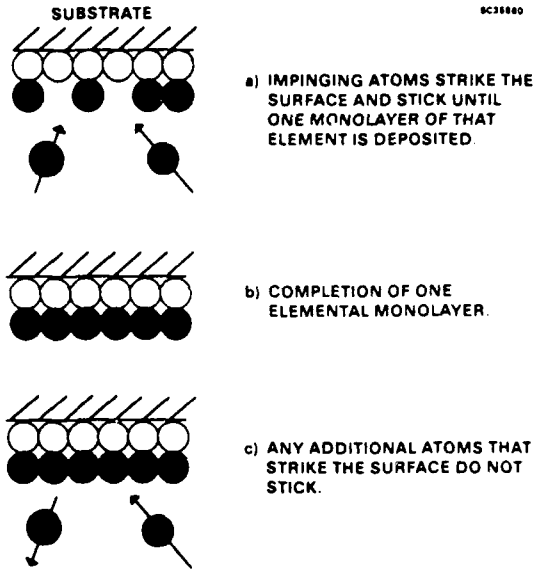

Fig. 1.3 Schematic representation of one-half of a cycle of the ALE growth process.

Chemisorption is a specific process that usually involves an activation energy. The result is that the process may be slow but it is not readily reversible. Physisorption, on the other hand, is usually a rapid process that is readily reversible and quickly reaches equilibrium. Chemisorption depends upon the energy released during the initial physisorption to reduce the activation energy. If this barrier is large, the rate of chemisorption at low temperatures will be slow and only physisorption will occur. At some higher temperature, chemisorption will be the dominant process and physisorption negligible. At this temperature only chemisorbed species are retained on the substrate surface (a single monolayer) while the

physisorbed (material > 1 monolayer) layers re-evaporate. This effect is the driving force behind the ALE technique and the reason why only one atomic layer of each element is deposited during a cycle. This also explains why substrate temperature is very important to this process.

The zinc chalcogenides (ZnS, ZnSe and ZnTe) are ideal materials for ALE deposition. The vapor pressure of the individual elements (Zn, S, Se and Te) are much higher than those of the II-VI compounds. This physical property can also be illustrated by considering the re-evaporation rate of the compounds and constituent elements as a function of temperature (Figs. 1.1 and 1.2). At ~ 350°C, the re-evaporation rates of the compounds (ZnS, ZnSe and ZnTe) are between 5 and 14 orders of magnitude less than those of the individual elements which comprise the compounds. This shows that monolayer growth is readily achievable with the compounds. Because of the stepwise growth process, ALE deposition of the materials offers particular advantages for the preparation of optical thin films such as rugate filters which require precisely controlled and uniform thickness.

Because of the equilibrium nature of the ALE growth process we expected the film deposition rates to be slow to moderate. Typical grow rates attained by other workers in this field are < 0.15 Å/s. If equilibrium is not established during the growth process, the excess material can be trapped on the surface by the next elemental beam, disturbing the film stoichiometry as well as affecting the thickness achieved per cycle. In an effort to maximize the growth rate, we looked at both thermal and laser evaporation as methods to get the elemental material from the source holders to the substrate. Laser evaporation is known to produce more energetic species in the evaporant plume[1,2] which can speed up the reaction at the film surface. An added advantage to laser evaporation is more efficient source material utilization. Thermal evaporation requires that the sources be kept heated while not actually in use, resulting in a low duty cycle for each crucible (e.g., Zn:50%, Se:25%, Te:25%). Laser evaporation had the advantage of almost instantaneous starting and stopping of evaporation when the laser is turned on or off. However, Zn and S proved to be incompatible with laser evaporation using 1.06 μm or 10.6 μm radiation. Zn is too reflective to achieve the desired evaporation rate while S is not absorbing enough. Because of this problem, we concentrated our efforts on making the thermal evaporation method as effective, efficient and rapid as possible while still maintaining the equilibrium growth conditions necessary for ALE.

2.0 THEORETICAL ACTIVITIES

The theoretical activities performed under this contract involved design and modeling of the rugate structure using different component systems. The initial design used ZnS and ZnSe but ZnS was replaced by ZnTe for reasons which will be discussed in the experimental section of this report.

2.1 Rugate Filter Design

The original rugate design for this project (discussed in the contract proposal) consisted of 16 layers per cycle; where the thinnest and thickest layers were 199Å of ZnSe and 4148Å of ZnS, respectively. This structure was designed to have a stopband wavelength (λ) of 10.6 μm, an average index (N_a) of 2.3 and an index excursion (N_p) of 0.2. The spatial period of a rugate filter (P) is given by

$$P = 0.5\ \lambda/N_a \qquad (1)$$

so a single cycle of this design is 2.17 μm thick. The index profile of a single cycle of this design is shown in Fig. 2.1. This profile takes advantage of the full available N_p by allowing the index excursion to range from pure ZnSe (n = 2.2) to pure ZnSe (n = 2.4). A sixty-cycle structure using this design requires a 130 μm-thick film which would have a bandwidth of 5% and a reflective optical density of > 3 (Fig. 2.2). Due to the unique growth mechanism of ALE, film thickness should be easily controlled in a nanometer range. To fully utilize this unique advantage, the filter was redesigned to increase the number of layers per cycle. The resulting design is a 100 layer per cycle structure in which the thinnest and thickest layers are 15Å of ZnSe and 433Å of ZnS, respectively. Index vs thickness for a single cycle of this design is shown in Fig. 2.3. The total thickness and the performance specifications are identical to that of the previous design (Fig. 2.2). This more "analog-like" structure was expected to have improved optical hardness characteristics.

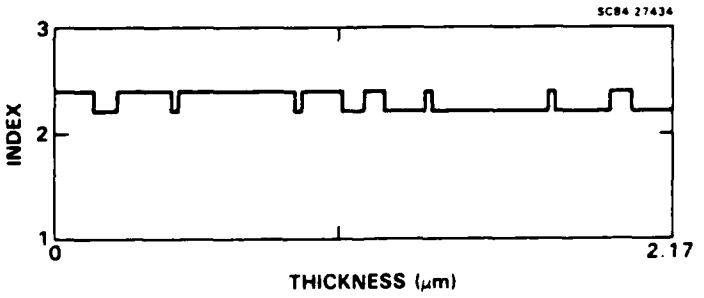

Fig. 2.1 Index profile of a single cycle of the ZnS/ZnSe rugate structure. This 16-layer group is equivalent in spectral response to a sine wave index variation.

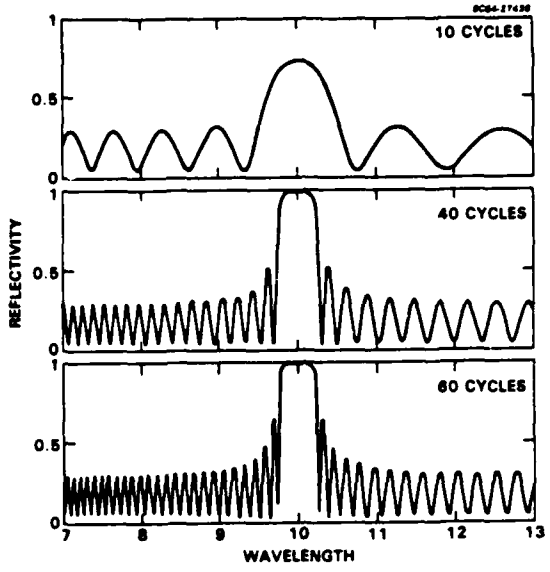

Fig. 2.2 Spectral reflectivity of 10 cycles (upper curve), 40 cycles (middle curve) and 60 cycles (lower curve) of the index variation shown in Fig. 2.1. The peak reflectivity of the 60-cycle structure is 0.9996.

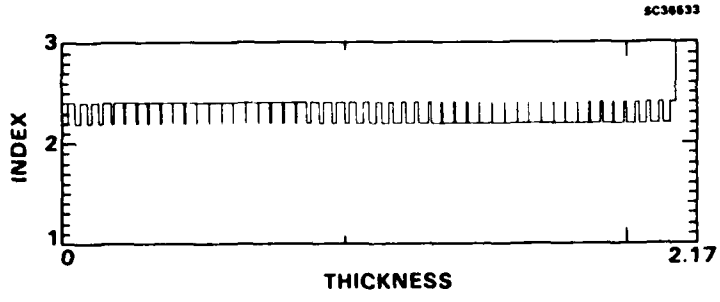

Fig. 2.3 Index profile of a single cycle of the "analog-like" design using ZnS and ZnSe. This structure consists of 100 layers and is equivalent in spectral response to the design in Fig. 2.1.

An alternative design consisted of 48 layers per cycle in which the thinnest and thickest layers were 20Å of ZnTe and 2209Å of ZnSe, respectively. The index profile of a single cycle of this design is shown in Fig. 2.4. Because of the higher average index (N_a = 2.542) of this structure, one complete cycle is 2.08 μm thick, compared to 2.17 μm for the ZnS/ZnSe case. This reduces the total thickness by ~ 5 μm over the original design. The spectral reflectivity of a 60-cycle structure using the new design is shown in Fig. 2.5. Because the index excursion is slightly higher (N_p = 0.28) for the ZnSe/ZnTe system, the bandwidth of the filter is ~ 6%.

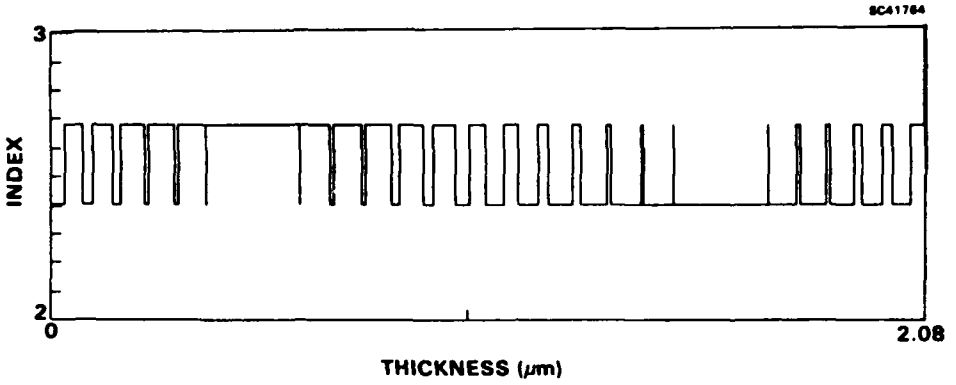

Fig. 2.4 Index profile of a single cycle of the ZnSe/ZnTe design. This structure consists of 48 layers.

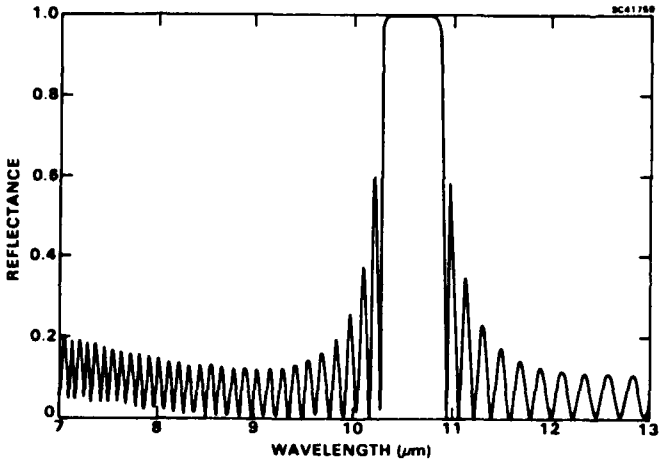

Fig. 2.5 Spectral reflectivity of 60 cycles of the index variation shown in Fig. 2.4. The optical density of this structure is 3.6.

A 200 layer per cycle rugate structure using ZnSe and ZnTe was also designed for a stop-band wavelength of 10.6 μm. The previous 48 layer-per-cycle design consisted of a complete excursion between the high- and low-index values (N_p = 0.28). Reducing the index excursion to 0.20 reduces the bandwidth from 6% to 4%. Figure 2.6 shows index of refraction versus film thickness for a single sinusoidal cycle. Sixty cycles of this design produces a structure which has a reflective optical density of ~ 3.6 and a total thickness of 126 μm. Figure 2.7 shows the reflectivity of the sixty cycle structure between 7 and 13 μm.

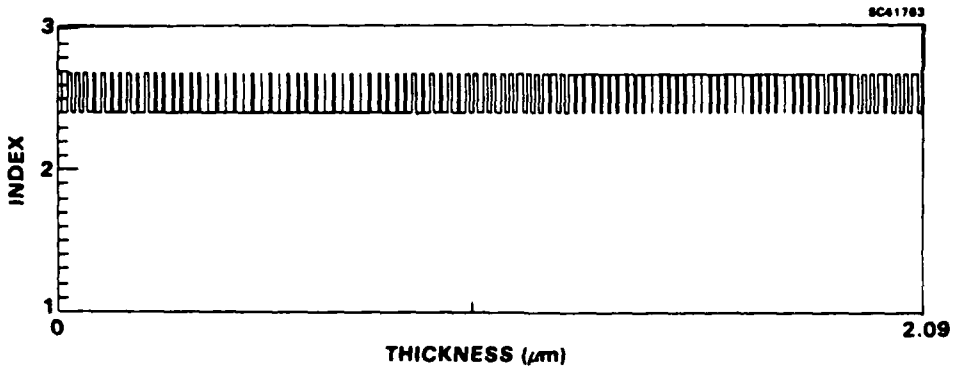

Fig. 2.6 Index profile of a single cycle of the ZnSe/ZnTe design. This structure consists of 200 layers.

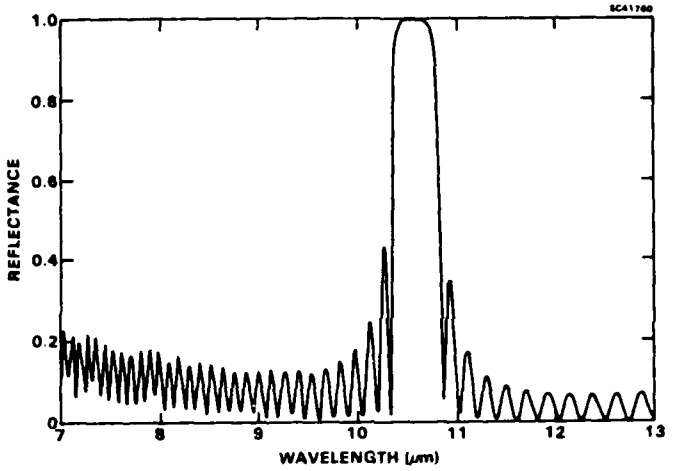

Fig. 2.7 Spectral reflectivity of 60 cycles of the index variation shown in Fig. 2.6.

3.0 EXPERIMENTAL ACTIVITIES

The experimental activities performed under this contract were in the areas of refinement and optimization of the ALE technique as applied to the zinc chalcogenides (including thermal evaporation and laser evaporation), and application of ALE to the fabrication of an IR rugate filter.

3.1 Instrumentation

The ALE deposition system (Fig. 3.1) consists of a 10 in. diameter ultra high vacuum system with a base pressure of 5×10^{-9} torr. The growth chamber is attached to a load-lock and an analysis chamber. The substrate holder is attached to a rod which can be translated from the load-lock into the growth chamber or into the analysis chamber. The load-lock allows a fast turnaround time between experiments by permitting the introduction of new substrates without venting the main chamber.

SC42543

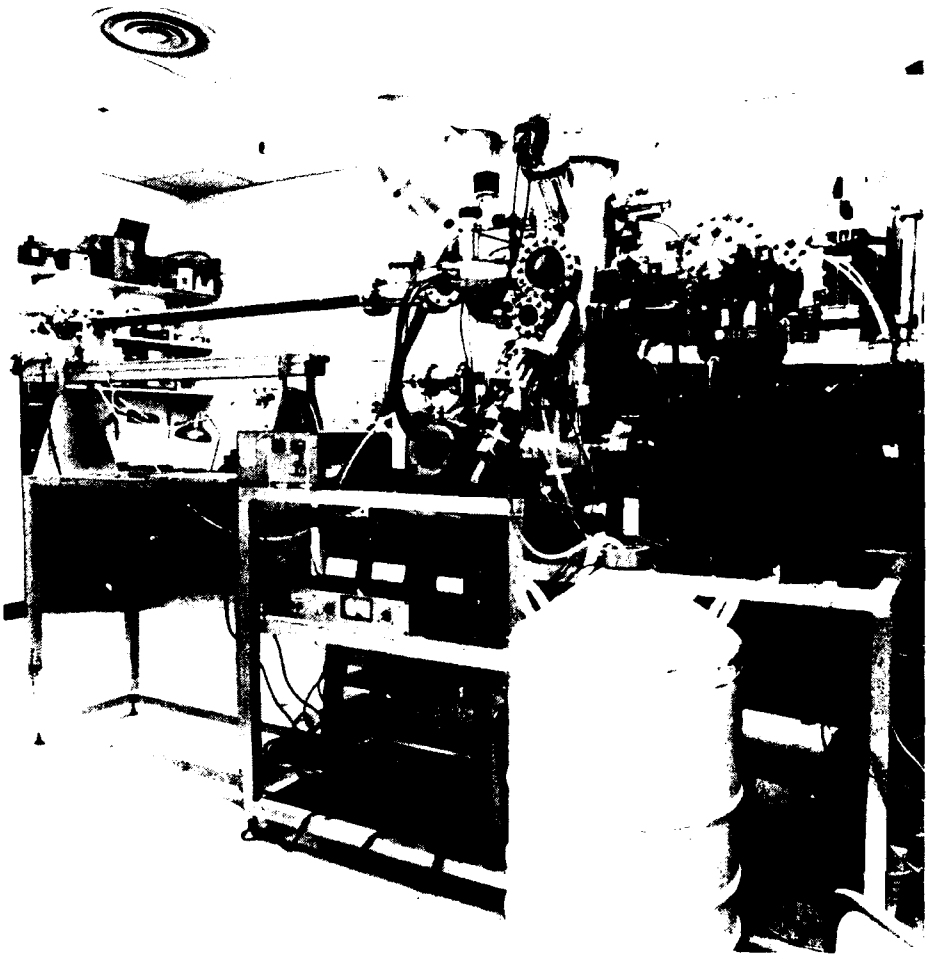

Fig. 3.1 Photograph of ALE deposition system including load-lock, growth chamber, and analysis chamber.

In the thermal evaporation mode, ZnS, ZnSe and ZnTe films are deposited from separate molecular beam sources containing Zn, S, Se, or Te. In the early stages of the program, each constituent element was alternately deposited onto the substrate by rotating a shutter, which contained a single 0.75 in. diameter orifice, into position over the appropriate effusion cell. A photograph of the thermal evaporation source flange is shown in Fig. 3.2. This flange is capable of containing three crucibles which have individual power and temperature monitoring feedthroughs. The crucibles are situated inside of a liquid nitrogen shroud designed to keep the base pressure at a minimum during depositions.

SC42542

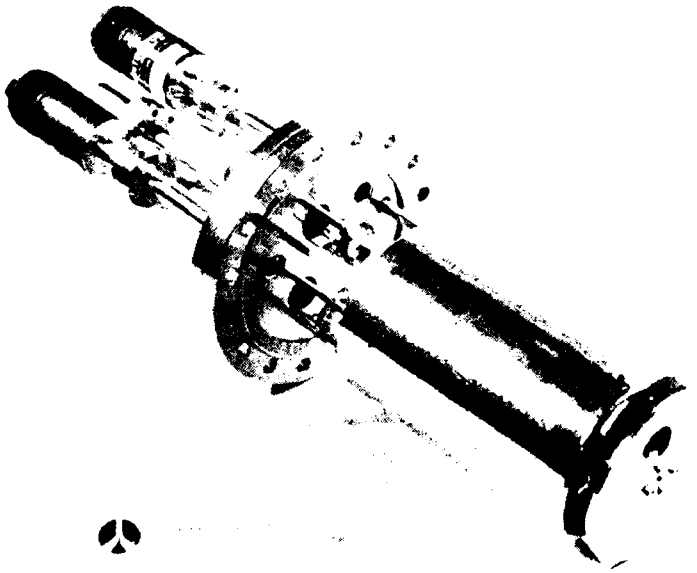

Fig. 3.2 Photograph of source flange used during thermal evaporation ALE depositions.

In later thermal evaporation experiments, a modified source flange was used in which the rotating shutter described above was replaced by three individual shutters (one over each crucible). This system utilized a ball-type linkage to couple a rotary motion feedthrough to each hinged shutter. Each shutter was individually actuated by means of a dc motor connected to its rotary motion feedthrough. The advantages of this type of design include conservation of source material by not allowing leakage of the element while it is not in use; decreasing the background pressure of the chamber during deposition; and decreasing the time needed to pump away excess material after deposition of each layer.

A separate flange was used for the laser-evaporated ALE experiments. In this system (shown in Fig. 3.3), the laser beam was adjusted to enter the vacuum system at a fixed position. A lens outside of the vacuum focussed the beam onto a source material holder containing an individual pocket for each element. The laser entered the source flange through a hole in the side of the liquid nitrogen shroud and the evaporated elements were directed through the hole in the top of the flange. Instead of rotating a shutter to expose a particular element as in the case of thermal evaporation, the source holder was rotated to move the appropriate element into the path of the laser beam. A pulsed Nd:YAG laser was used to evaporate the source materials. It was capable of delivering 800 mJ (at 1.06 μm) in a 10 ns pulse at a rep rate of 40 Hz.

SC42541

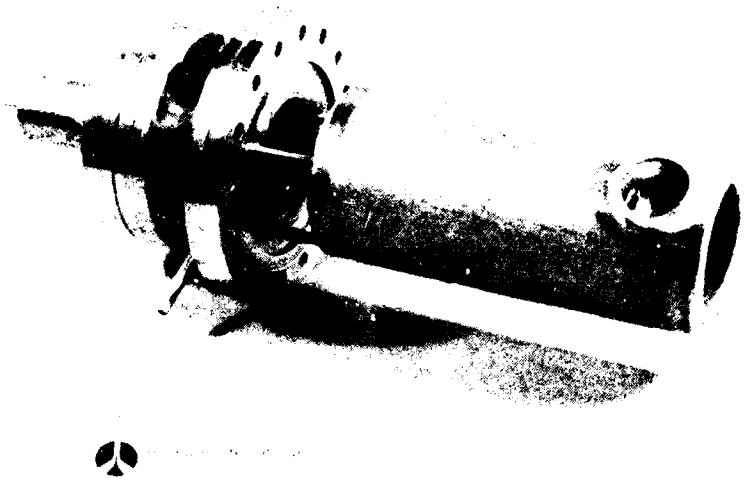

Fig. 3.3 Photograph of source flange used during laser evaporation ALE depositions.

The evaporation control system (Fig. 3.4) used with the rotating orifice thermal evaporation flange and the laser evaporation flange consisted of a Compumotor model 2100 stepper motor controller which was interfaced via an RS232 serial line to an IBM-XT computer. The stepper motor has its own command language through which a wide variety of functions can be executed. The control program, running from the IBM-XT, is responsible for calculating the number of atomic layers which make up each compound layer. This number is a function of the lattice constant of the material as well as the ALE growth direction. After calculating the appropriate values for the entire rugate cycle, the program downloaded the information necessary to run the stepper motor; received feedback from the stepper motor controller concerning the status of the shutter movement; and kept track of the rugate cycle number, compound layer number, and atomic layer number which was currently being deposited.

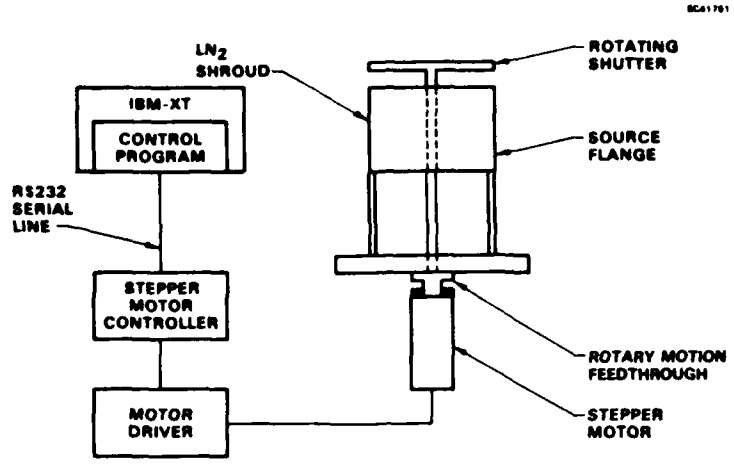

Fig. 3.4 Schematic diagram of the evaporation control system used during thermal evaporation with the rotating orifice shutter and during laser evaporation depositions.

In the case of the individually controlled shutter system, a computer-controlled relay board activated a dc motor on each rotary motion feedthrough (Fig. 3.5). The computer communicated with the relay card via a digital I/O line. The dc motors were fitted with two limit switches which opened the electrical circuit and stopped the feedthrough rotation at the appropriate opened or closed position. The original control program was modified to send the correct commands to the relay board to activate the shutter system. Except for monitoring the amount of source material remaining in the effusion cells or in the laser evaporation container, the process was completely automated.

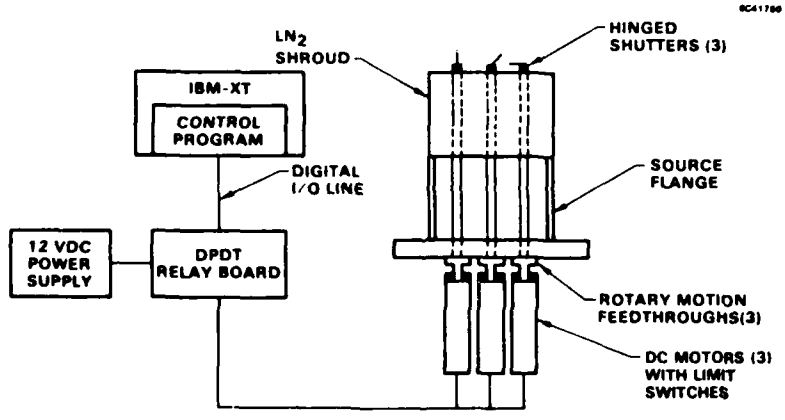

Fig. 3.5 Schematic diagram of the evaporation control system used during thermal evaporation with individually controlled shutters.

3.2 Thermal Evaporation

ALE is a new growth technique, and material development was a crucial part of this program. Preliminary work in this area was performed under Rockwell International IR&D prior to the contract start. This work resulted in the definition of a range of growth parameters (substrate temperature, effusion cell temperature, and duration of exposure of the substrate to each element) under which high quality epitaxial films of ZnS or ZnSe were deposited. As a result of the progress made during these preliminary experiments, we concentrated our initial efforts on determining the optimum growth parameters for the ALE growth of zinc chalcogenide films. Because of the inherently slow growth rate of the ALE process, we also wanted to determine the maximum cycle speeds under which equilibrium growth conditions could still be achieved. In addition, to efficiently and effectively fabricate an IR rugate filter using ALE, a single set of growth parameters must be determined which will give the best results for the two compounds used in the optical structure. The last important task in the development stage of the contract was to examine the unique features of ALE, the monolayer growth mechanism, film thickness control, and film uniformity.

ALE films of ZnS, ZnSe and ZnTe were grown on (100)-oriented GaAs substrates from thermal evaporation sources containing the constituent elements. A useful test to confirm the monolayer growth of ALE is to plot thickness versus the number of cycles (1 Zn layer, 1 group VI layer) completed. If the deposition proceeds in a stepwise manner, then the slope of the line should be a/2 for the (100) growth direction; where a is the lattice constant of the zincblende material. Figure 3.6 shows such a graph for ZnSe on GaAs(100). The solid line represents ideal growth (2.83 Å/cycle) and is almost identical to the observed data. Similar plots for ZnS and ZnTe on GaAs(100) are shown in Figs. 3.7 and 3.8, respectively. For ZnS, ideal growth is 2.70 Å/cycle and 2.05 Å/cycle for ZnTe. Again, the film thickness is extremely close to the expected values. Film thickness was measured using a Dektak II stylus profilometer, spectrophotometric data, and ellipsometric analysis. These results clearly show that only one molecular layer is deposited during a single shutter cycle.

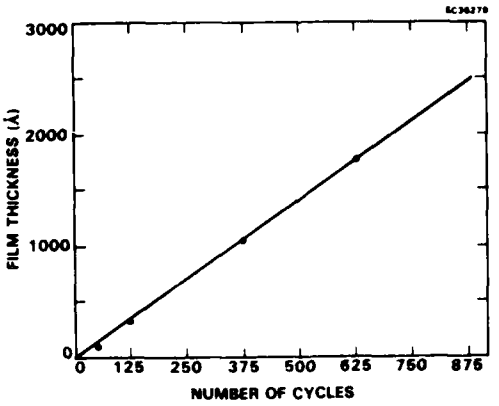

Fig. 3.6 Film thickness vs the number of completed cycles for ZnSe grown on GaAs(100) by ALE. The solid line represents ideal growth for this system (2.83 Å/cycle). The data points closely follow that of the idealized growth.

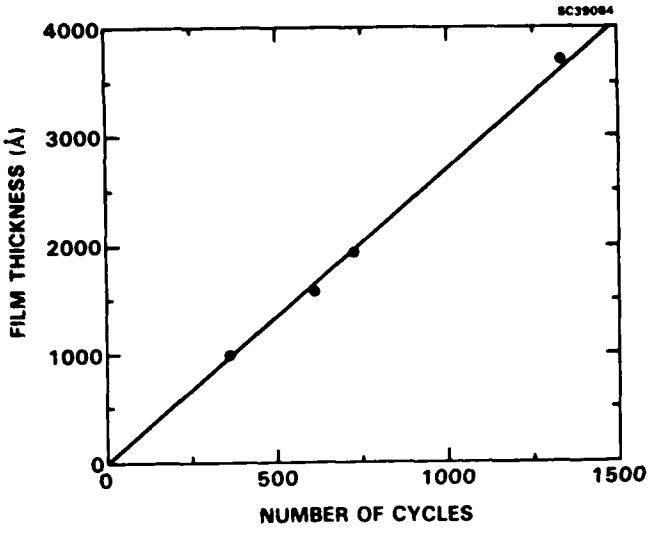

Fig. 3.7

Film thickness vs the number of completed cycles for ZnS on GaAs(100). In this system, the ideal growth is 2.70 Å/cycle.

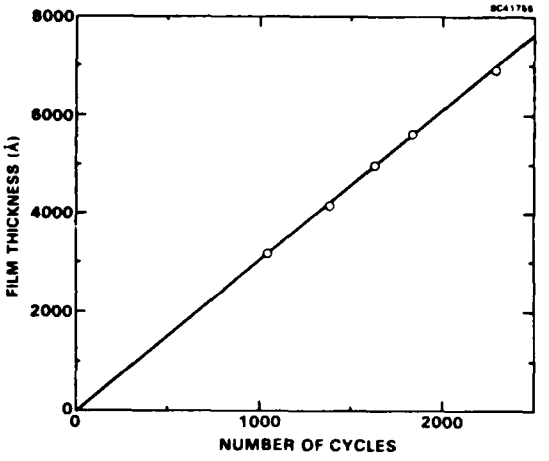

Fig. 3.8

Film thickness vs the number of completed cycles for ZnTe on GaAs(100). In this system the ideal growth is 3.05 Å/cycle.

The optical properties of the zinc chalcogenide films were characterized using spectrophotometry and ellipsometry. Transmission data, taken from 0.88 to 2.6 μm (Figs. 3.9-3.11), showed that the thin films absorbed very little in this spectral region. Comparing the transmission of the film covered substrates to that of clean GaAs gives an upper limit of ~ 1 cm^{-1} for the absorption coefficient of all three compounds. Data obtained from a rotating-analyzer ellipsometer (at 0.63 μm) in addition to spectrophotometric data were used to calculate the index of refraction of the ALE-grown films. Values of 2.35, 2.55 and 2.96 were obtained for ZnS, ZnSe and ZnTe, respectively; which are in excellent agreement with bulk values of 2.345, 2.581 and 2.967, respectively.[13]

Information on the film crystal structure was obtained by x-ray diffraction (XRD) using a Phillips instrument utilizing CuK_α radiation to measure peak position in the range $20° < 2\theta < 100°$. Initial scans of the clean (100)-oriented GaAs substrates showed only the (400) peaks at ~ 66.4°. After the deposition of 5408Å of ZnS, the XRD spectrum showed a peak due to ZnS (200) planes as well as the original GaAs substrate peaks (Fig. 3.12). The full-width at half-maximum of the ZnS peak was 0.2°, indicating high crystalline quality.

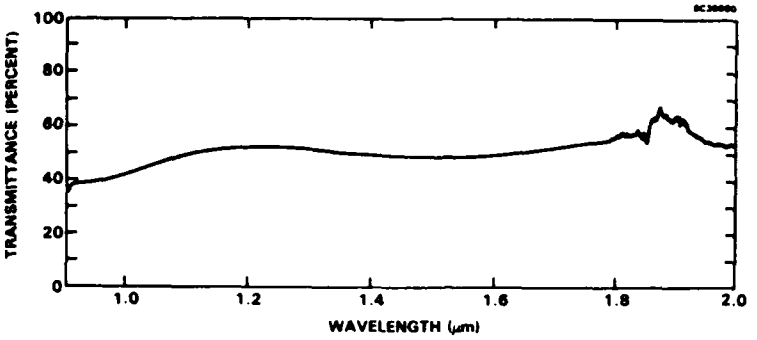

Fig. 3.9 Spectral transmission of a 4670 Å-thick film of ZnS on GaAs(100).

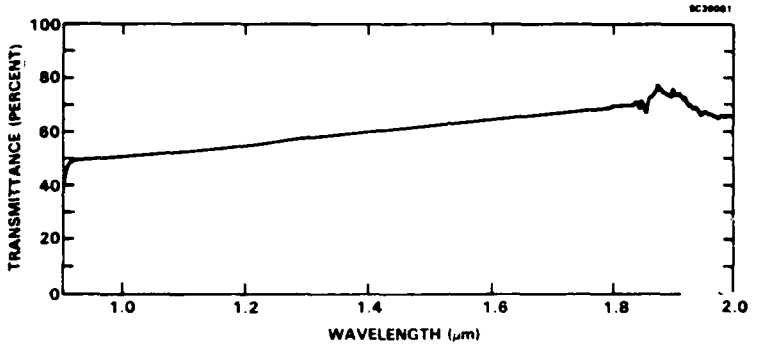

Fig. 3.10 Spectral transmission of a 7670 Å-thick film of ZnSe on GaAs(100).

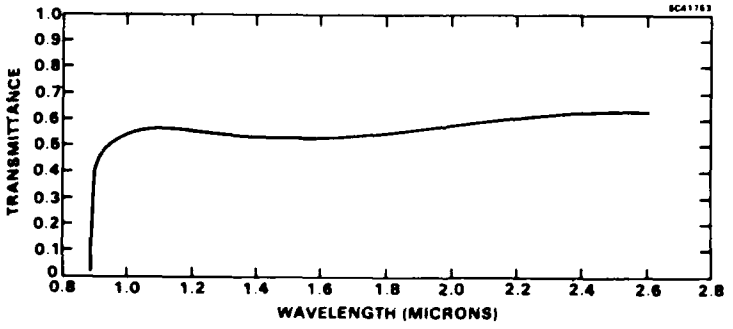

Fig. 3.11 Spectral transmission of a 2994 Å-thick film of ZnTe on GaAs(100).

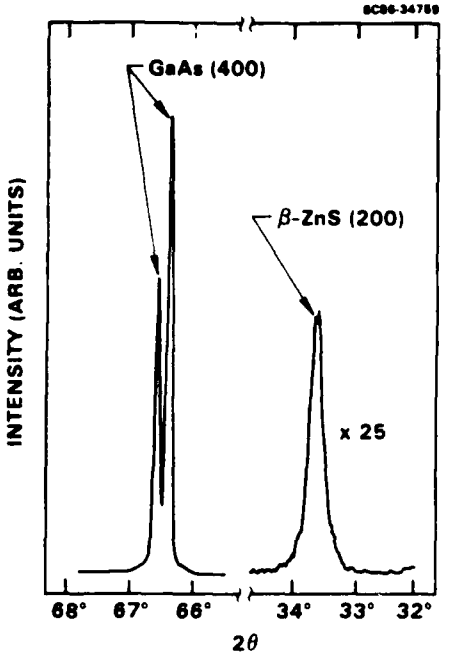

Fig. 3.12

XRD spectrum of ZnS on GaAs(100). The only peaks present are those of the substrate (~ 67°) and the [100] oriented ZnS film (~ 34°).

XRD spectra were also taken of ZnSe films of varying thicknesses on GaAs(100), but because of the close lattice match of these two materials (ZnSe: a = 5.669Å; GaAs: a = 5.653Å), only a slight broadening of the GaAs substrate peak was seen (Fig. 3.13). However, the intensity of the (400) peak is the same for both clean and ZnSe-coated samples. If the ZnSe films had been amphorous, thus exhibiting no diffraction peaks, the intensity of the substrate peak of the film-covered sample would have been measurably reduced. No other diffraction peaks were observed, indicating that the ZnSe film growth was in the same direction as the substrate.

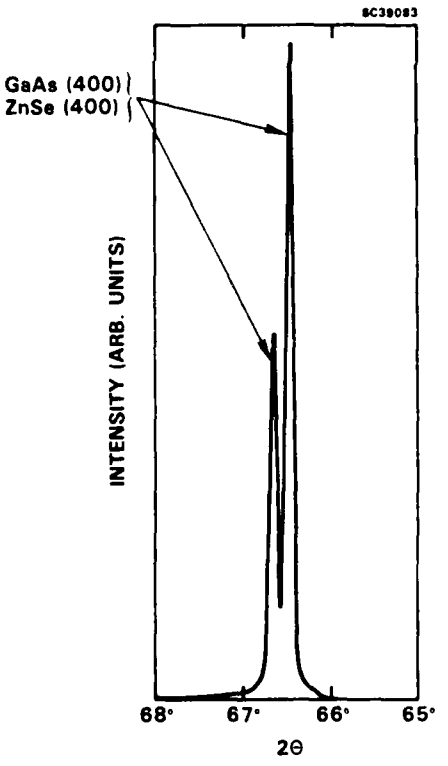

Fig. 3.13

XRD spectrum of ZnSe on GaAs(100). Because of the small lattice mismatch (~ 0.2%) between the film and the substrate, the XRD peaks of the two materials are superimposed.

Figure 3.14 shows the XRD spectrum of a 3000 Å-thick film of ZnTe on GaAs(100). In this instance the ZnTe peak (60.6°) is visible because it is not as well lattice-matched to GaAs. The low intensity GaAs(400) peaks at 63° and 63.5° are due to diffraction of $WL\alpha$, and $WL\alpha_2$ radiation, respectively. The ZnTe peak is from the CuK_α radiation. The full-width at half-maximum of the ZnTe diffraction peak is ~ 0.4° indicating good crystalline quality. The XRD data of all three compounds are consistent with epitaxial growth on a single crystal substrate.

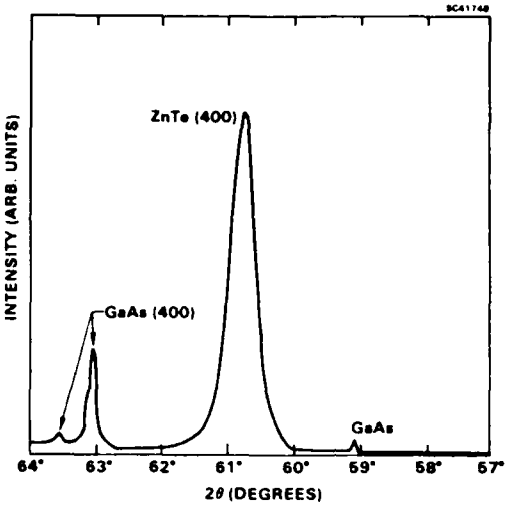

Fig. 3.14 XRD spectrum of ZnTe on GaAs(100). The only peaks present are those of the substrate (~ 59°, ~ 63°) and the [100] oriented ZnTe film (~ 61°).

Laue x-ray backscattering was also performed on clean and film-coated substrates. This technique enables one to compare the crystal orientation of the epitaxial layers to that of the single-crystal substrate. Since this technique is inconclusive for very thin films, only samples where the film thickness was ≥ 5000Å were examined. (100)-oriented zincblende materials exhibit a four-fold symmetric pattern such as the one shown in Fig. 3.15. This identical pattern was seen on clean GaAs and on substrates containing ZnS, ZnSe or ZnTe films. The lack of change in the pattern is due to the fact that a "white" x-ray source was used; so when the orientation of the film and the substrate is identical, the diffraction spots of the two materials are superimposed. The absence of a second set of four-fold symmetric spots (rotated with respect to the substrate spots) indicates that the zinc chalcogenide films were also grown in registry with the GaAs substrate (i.e., the film lattice is not rotated with respect to the substrate lattice). These data in conjunction with the XRD results indicate that the ALE-grown ZnS, ZnSe and ZnTe films were high quality epitaxial layers which grow in the same direction and orientation as the substrate.

SC42540

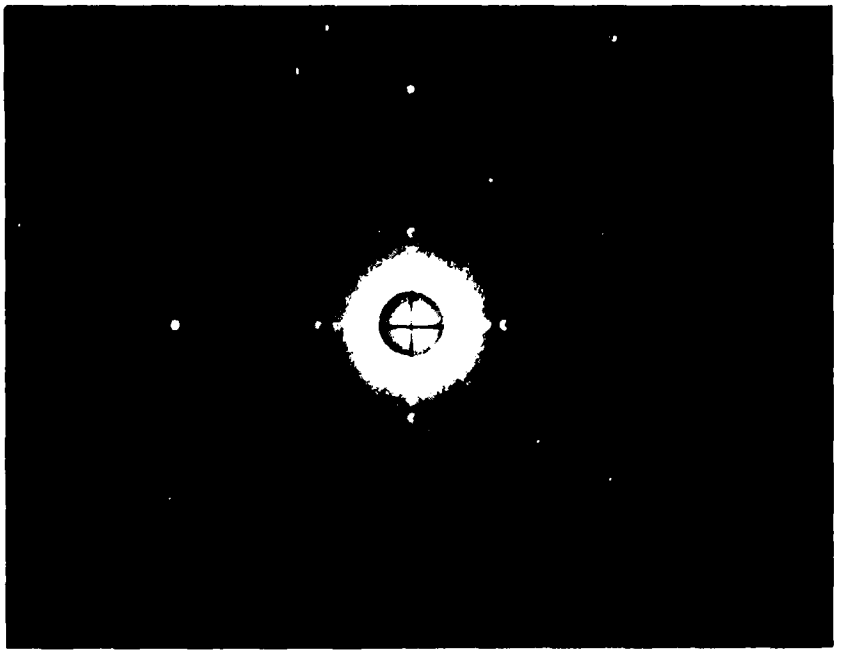

Fig. 3.15 Typical Laue x-ray backscattering photograph of a (100)-oriented zincblende structure. This pattern was seen for clean GaAs(100), and on GaAs substrates after depositions of (> 5000Å) ZnS, ZnSe and ZnTe.

The zinc chalcogenide thin films, which were described above, were grown over a range of growth conditions. For example, the substrate temperature for the ZnS and ZnSe films were in the range of 300-400°C and 275-375°C, respectively. After establishing the quality of these ALE-grown thin films, experiments were performed to determine what single set of growth parameters would optimize the growth of both ZnS and ZnSe. The optimum parameters for each individual compound are not necessarily identical, so intermediate values which work best for both compounds were determined. This was accomplished by looking at film quality, thickness uniformity, and thickness control as a function of growth parameters. The optimum temperatures of the Zn, S, and Se effusion cells, which were determined by growing the individual compounds, can be used in the rugate fabrication because the temperature of each cell can be individually controlled. Likewise, the amount of time the substrate is exposed to each element can be the same during rugate fabrication as in the growth of each compound. However, the optimum substrate temperature for growing ZnS is not the same as that for ZnSe. The most effective temperature for the filter structure would be a value intermediate between that of the individual compounds. A series of ZnS and ZnSe films were grown in the temperature range 325-375°C. These films were characterized to determine at what single temperature the two compounds were most bulk-like in their properties. This temperature, as well as the growth parameters previously determined, were deemed the optimum parameters for the ALE growth of both ZnS and ZnSe and are listed below:

a. Substrate temperature: 340°C
b. Zn crucible temperature: 330°C
c. S crucible temperature: 90°C
d. Se crucible temperature: 205°C
    i 2.5 s S(Se) exposure
    ii 0.5 s pause
    iii 2.5 s Zn exposure
    iv Repeat above

A similar set of experiments was performed to determine the optimum substrate temperature for the ZnSe/ZnTe system. Since the vapor pressure of ZnTe is higher than that of ZnS, a lower range of temperatures (285-345°C) was examined. The optimum parameters for ALE growth at ZnSe and ZnTe multilayer structures are as follows:

a. Substrate temperature: 305°C
b. Zn crucible temperature: 285°C
c. Se crucible temperature: 195°C
d. Te crucible temperature: 295°C
e. Timing scheme:
    i 3.3 s Se exposure
    ii 1.0 s pause
    iii 3.3 s Zn exposure
    iv 1.2 s pause
    v 3.3 s Te exposure
    vi 1.8 s pause
    vii 3.3 s Zn exposure
    viii Repeat (i) - (vii).

3.3 Laser Evaporation

Although thermal evaporation is a simple, dependable technique to get material from a crucible to the substrate, it poses certain limitations on the ALE process. The two most serious setbacks are crucible duty cycle and slow growth rate. For these reasons, experiments were conducted to determine the feasibility of using a laser to evaporate the elements during ALE depositions. Laser evaporation is known to produce more energetic species in the evaporant plume than more conventional techniques, in addition to completely dissociating most molecular species.[12] These excited atoms could decrease the amount of time needed to reach equilibrium conditions during the ALE process, thus allowing a faster cycle time. In the ALE process, only one element is deposited at a time. Because of the lag time associated with heating and cooling a large thermal mass such as a crucible, it cannot be turned off when not in use. Thus, material from one elemental source continues to evaporate when that element is not needed. Laser evaporation solves this problem since evaporation stops almost instantaneously when the laser beam is turned off. If one laser is used to evaporate material during ALE depositions, then source material is fully utilized since it is not being evaporated when not needed.

The feasibility of using laser evaporation with the zinc chalcogenides was first investigated by conducting evaporation tests of the different elements outside of the vacuum system. This was accomplished by placing a small target of Zn, Se, Te or S in quartz containers and exposing the element to the laser beam. A pulsed Nd:YAG laser capable of delivering

800 mJ in a 10 ns pulse at a rep rate of 40 Hz was used in this study. However, for the initial tests, a rep rate of 10 Hz and a pulse width of 100 ns was used. In the case of Se, reddish material could be seen evaporating from the target with each laser pulse. We determined that effective Se evaporation can be achieved with laser energies between 400 and 700 mJ/pulse. Elemental Te evaporated much more readily due to its extremely large absorption coefficient (10^5 cm^{-1}) at 1.06 μm. Laser energies between 100 and 300 mJ/pulse produced large Te fluxes. Elemental S could not be evaporated even with the laser at full power. Frequency doubling the laser light was used in an attempt to create more free carriers, thus increasing the absorption at 1.06 μm. This did not work because the band gap of S is 3.6 eV, so creation of free carriers with 0.53 μm radiation is still a multiphoton process. Elemental Zn required almost full power to achieve any sign of evaporation, due to its high reflectivity at 1.06 μm. This low absorptivity would require long exposure times to ensure that sufficient Zn reaches the substrate. Because Zn is required for any of the three compounds, Zn evaporation would become the bottleneck step of the process. It was finally determined that elemental laser evaporation was unsuitable for our material system and that thermal evaporation would be the method of choice.

3.4 Optical Structures

Based on the results of the laser evaporation experiments, the decision was made to concentrate on thermal evaporation for the contract duration. However, instead of returning to the originally proposed ZnS/ZnSe system we continued to work with ZnSe and ZnTe, for several reasons. Elemental S has an extremely high vapor pressure making it difficult to control the flux at low crucible temperatures. Te, on the other hand, has the lowest vapor pressure of these group VI elements, making it highly suitable for thermal evaporation and easier to control. In addition, the ZnSe/ZnTe system has a higher average index (N_a = 2.54). The result is that each sinusoidal cycle is thinner than in a lower N_a system. Since the growth rate of ALE is slow, this is an important consideration. The higher N_a also means that the same optical density can be achieved with fewer cycles than a system with low N_a. Lastly, the optimum substrate temperature of the ZnSe/ZnTe system was lower, making it more compatible with deposition on any temperature-sensitive devices or substrates.

We attempted to fabricate two types of optical structures during this part of the contract. Initially, quarter-wave stacks of between 2 and 6 alternating layers of ZnSe and ZnTe were deposited. These structures have fewer interfaces compared to a rugate filter, making it easier to interpret the results of characterization techniques such as XRD, Laue x-ray backscattering and spectrophotometry. Rugate structures of 3, 5 and 8 sinusoidal cycles (40 layers/cycle) were attempted after the quarter-wave stack experiments.

3.4.1 Quarter-Wave Stacks

Quarter-wave stacks with stopband wavelengths of 1.0 or 1.3 μm were grown using ALE. The 1.0 μm structures consisted of alternating layers of ZnSe and ZnTe which were 1006Å and 855Å, respectively. The ZnSe and ZnTe layer thickness was increased to 1302Å and 1189Å, respectively, in the 1.3 μm filters. The total number of alternating layers in both types of structures ranged from 2 to 6.

The measured and predicted transmittance of a 1.0 μm structure is shown in Fig. 3.16. This spectrum is typical of the quarter-wave stacks in that the average transmittance is ~ 0.45

indicating little absorption in the ZnSe and ZnTe layers. The XRD spectrum of the same multilayer structure is shown in Fig. 3.17. The ZnSe peak (~ 66°) is once again covered by the GaAs substrate peak but the diffraction peak due to the (400) planes of ZnTe is seen at ~ 61°. This peak is much broader and has a distinct shoulder compared to the previous single layer ZnTe films (Fig. 3.14). The shoulder occurs at higher 2θ values indicating a movement to smaller interplanar spacings. This is probably the result of compressive stress on the ZnTe film due to the smaller lattice constants of the GaAs substrate and the ZnSe films. The width of the diffraction peak indicates that there is a distribution of lattice constants through the ZnTe layers.

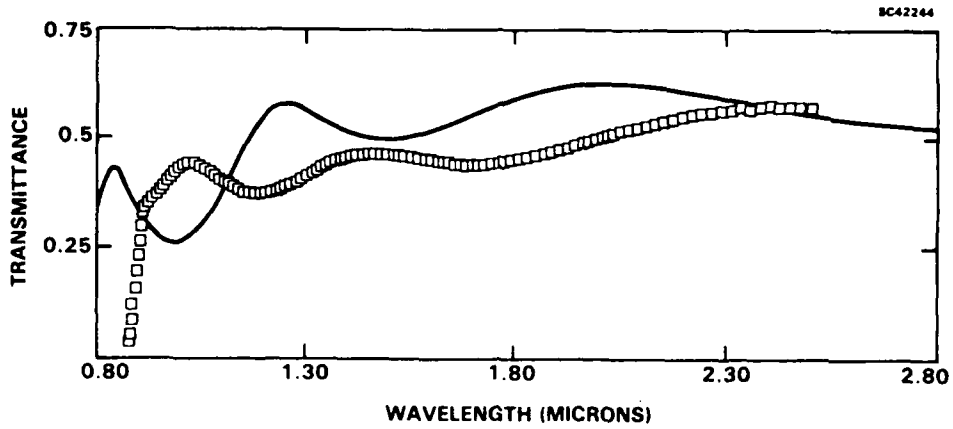

Fig. 3.16 Measured (squares) and predicted (smooth line) spectral transmission of a 6- layer quarter-wave stack of ZnSe/ZnTe at 1.0 μm.

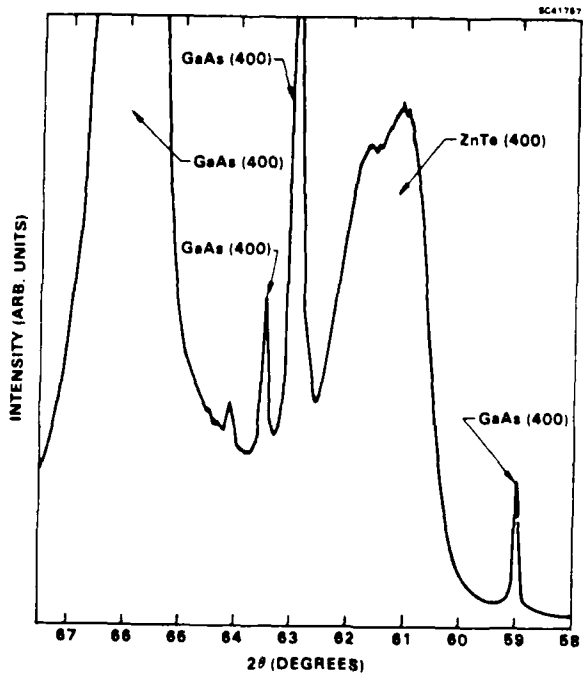

Fig. 3.17

XRD spectrum of the 6-layer ZnSe/ZnTe quarter-wave stack shown in Fig. 3.16.

The measured thicknesses of the multilayer quarter-wave stacks were compared with the predicted thickness based on the number of atomic layers of each compound deposited. Of the six structures fabricated during this phase of the contract, the measured thickness varied from 10% less than predicted to 5% greater than predicted. Since the uncertainty of thickness values obtained from the Dektak II stylus profilometer are sensitive to the slope of the step being measured as well as the roughness of the film and the substrate, the measured values were considered to be within experimental error of those expected.

One of the quarter-wave stacks was cleaved and a scanning electron microscope was used to perform elemental analysis (EDX) from an edge-on view of the sample. This structure should be composed of 50% (atomic) Zn, 29% Se and 21% Te, based on the expected thickness of the layers comprising the structure. The measured composition was 49% Zn, 39% Se, 12% Te indicating a deficiency of Te. It was not known whether the deficiency was due to a cumulative error in each of the ZnTe layers or a large error in a single layer.

3.4.2 Rugate Structures

After the completion of the quarter-wave stack experiments, rugate structures consisting of 3, 5 and 8 sinusoidal cycles were attempted. These structures were comprised of 40 layers/cycle. The 3- and 5-cycle structures were designed to have stopband wavelengths at 1.06 μm while the 8-cycle structure was at 1.5 μm. The design was derived from a 60 layer per cycle structure. Any individual layer which was less than 6Å was discarded and the two adjacent layers were combined. This procedure resulted in 40 layers/cycle where the thinnest layer was ~ 6Å and the thickness layer was ~ 362Å. The average index (N_a) of each design was 2.628 while the index modulation (N_p) was 0.29.

Because of the slow growth rate (0.40 Å/s), the five-cycle rugate was deposited over a two-day period. The first two cycles were completed on the initial day and the final three cycles were deposited on the second day. The substrate and the film were left at the growth temperature (305°C) and under vacuum during the time between the depositions. The film was lightly ion-bombarded (20 min of 0.5 kV Ar^+) to clean off any contamination resulting from the delay before the second half of the deposition. The expected thickness of the five-cycle structure was 1.01 μm. The actual thickness was 1.02 μm as measured by the stylus profilometer. The measured and predicted transmittance of this structure is shown in Fig. 3.18. A minimum is seen at 1.06 μm but it is distorted due to the large dispersion and cutoff of the GaAs structure at 0.9 μm. The average transmittance of the structure is ~ 0.6 from the band edge out to 2.5 μm, indicating little absorption in the ZnSe and ZnTe layers.

The XRD spectrum of this structure showed no sign of the ZnTe feature seen in the quarter-wave stacks (Fig. 3.17). In addition, EDX measurements obtained by cleaving the sample and viewing on edge indicated the film composition was 50% Zn, 47% Se and 3% Te, far short of the 50:28:21 ratio which was expected. It is not known how the total film thickness can be less than 1% from the predicted value and the stoichiometry be so different. This behavior follows the trend seen in the quarter-wave stacks but to a much greater extent.

The eight-cycle rugate structure was moved to an arbitrary stopband wavelength (1.5 μm) to avoid the problems of large dispersion and cutoff of the GaAs substrate in the 1.06 μm region. This structure was grown over a five-day period by the same technique as described above. The expected thickness of this filter was 2.308 μm while the measured thickness was

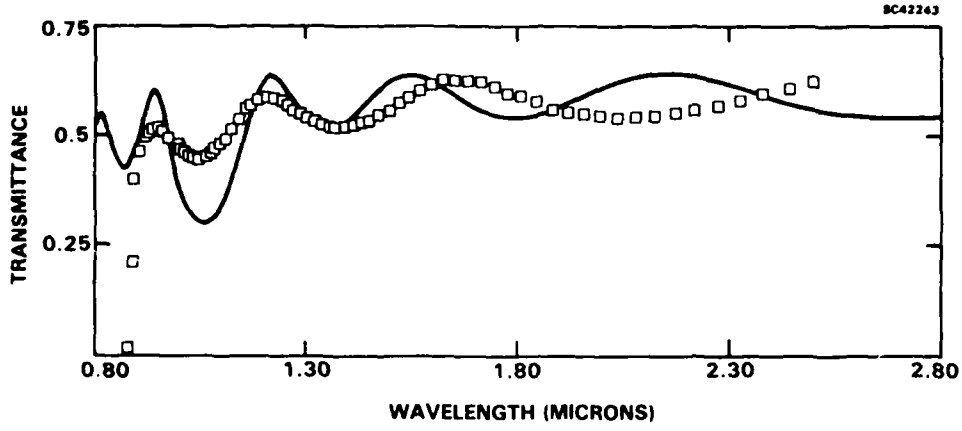

Fig. 3.18 Measured (squares) and predicted (smooth line) spectral transmission of a 5-cycle rugate filter with a stopband wavelength of 1.06 μm.

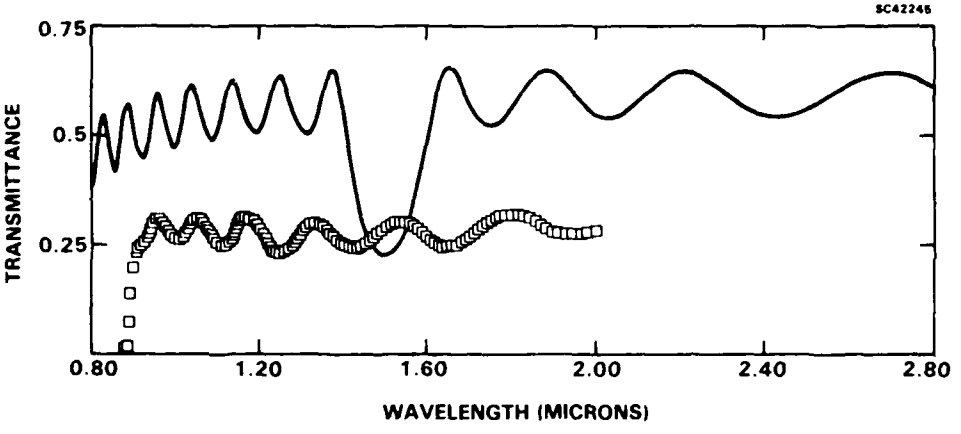

Fig. 3.19 Measured (squares) and predicted (smooth line) spectral transmission of an 8-cycle rugate filter consisting of ZnSe and ZnTe with a stopband wavelength of 1.5 μm.

2.309 μm. The measured and predicted transmittance of the structure is shown in Fig. 3.19. Although there is a minimum at ~ 1.45 μm, the overall spectrum is far different than expected, such as an average transmittance of only ~ 0.3. The XRD spectrum of this structure is shown in Fig. 3.20. Once again there is no trace of a ZnTe feature, but there is a shoulder at ~ 31.2° which is indicative of ZnSe. This feature (due to the 200 planes of ZnSe) may be visible because of the tensile stress felt by the ZnSe layers due to the ZnTe. EDX measurements showed the film composition to be 50% Zn, 45% Se and 5% Te. Once again the layers of ZnTe are much thinner than expected.

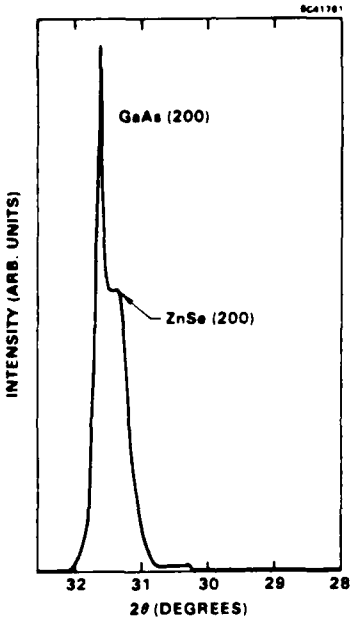

Fig. 3.20

XRD spectrum of the 8-cycle rugate filter shown in Fig. 3.19.

Following completion of the technical effort, fundamental analysis work was performed under a generic IR&D program. This included more in-depth analysis of rugate and quarter-wave structures fabricated under this program and growth and analysis of simple alternating layer samples to study relative nucleation rates. The following IR&D results are reported here for completeness. X-ray photoelectron spectroscopy (XPS) was used to obtain a quantitative measure of the relative stoichiometry of the film. Figure 3.21 shows a survey spectrum of the rugate structure with binding energies between 0 and 1200 eV. The important features in this spectrum are enlarged in Figs. 3.22 - 3.24. Quantitative analysis was performed using the relative peak areas of the Se 3d feature (60 eV; Fig. 3.22), the Te $3d_{5/2}$ and $3d_{3/2}$ features (578 eV, 588 eV; Fig. 3.23) and the Zn $2p_{3/2}$ and $2p_{1/2}$ features (1027 eV, 1052 eV; Fig. 3.24). After correcting for the relative cross section of each photoelectron excitation

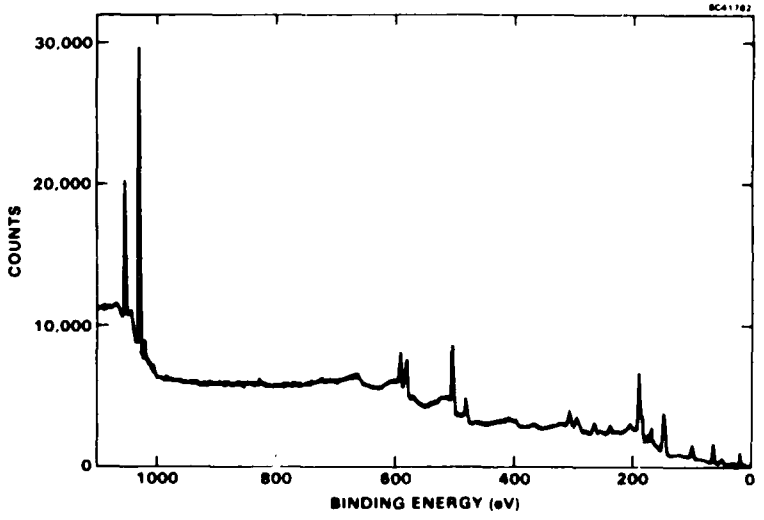

Fig. 3.21 XPS survey scan of the 8-cycle rugate structure.

and the relative escape depth of the emitted photoelectron, a ratio of 51% Zn, 32% Se and 17% Te was obtained. Since the interaction depth of the XPS experiment (~ 30Å) is much less than that of EDX (~ 1 μm), the results of the two experiments do not necessarily disagree. However, the fact that the ZnTe portion of the multilayer structure is too thin is quite evident in both results.

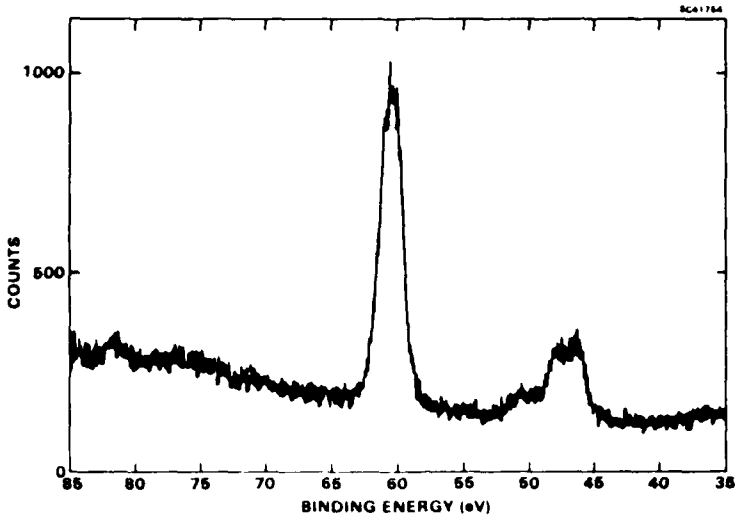

Fig. 3.22 XPS spectrum showing the peak due to Se 3d electrons (~ 60 eV).

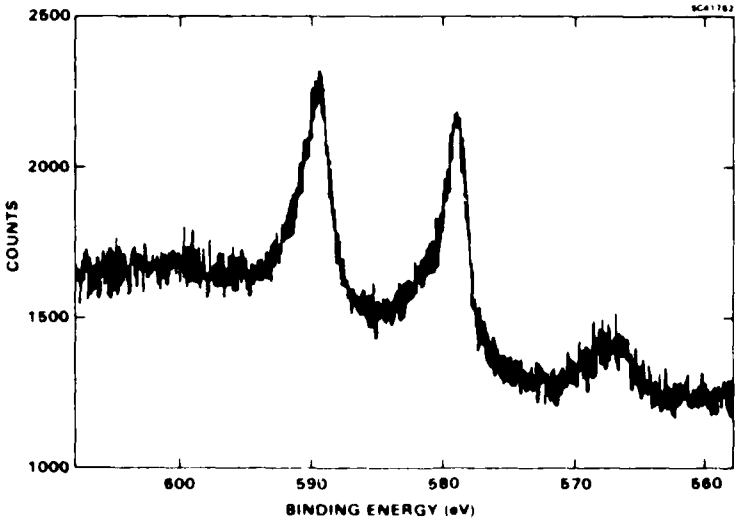

Fig. 3.23 XPS spectrum showing the peaks due to Te $3d_{5/2}$ (~ 578 eV) and Te $3d_{3/2}$ (~ 588 eV) electrons.

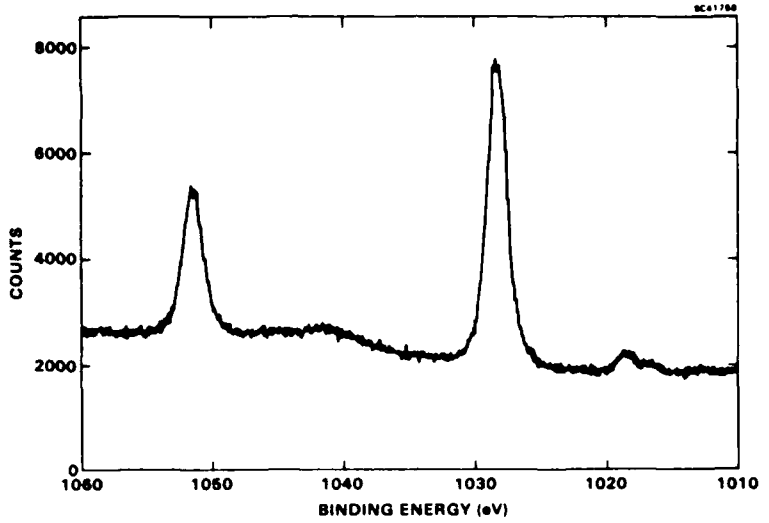

Fig. 3.24 XPS spectrum showing the peaks due to Zn $2p_{3/2}$ (~ 1027 eV) and Zn $2p_{1/2}$ (~ 1052 eV) electrons.

Exactly why the multilayer optical structures grown by ALE did not perform as expected is not known at this time. However, several points are very clear. All of the elemental analysis techniques performed on the quarter-wave stacks and the rugate structures indicate that there is a problem with the ZnTe layers. This shortage of ZnTe is much more pronounced in the rugate structure than in the quarter-wave stacks. One explanation of this result, which is consistent with the observed data, is that there is a problem with the nucleation of ZnTe on an existing ZnSe layer. The quarter-wave stacks have far fewer ZnTe/ZnSe interfaces, making the effect much less noticeable than in the rugate structures. Related work on ZnSe/ZnTe multilayered structures grown on InP(001) indicate that nucleation of the Te layer on an existing ZnSe film takes longer than on a ZnTe film. This is probably due to the interaction of the evaporant species (Te_2) with the film surface. Another possible explanation is that the optimum growth parameters determined for the single compound films are not applicable to the multilayer structure. Substrate temperature plays a vital role in the ALE process, so if the temperature is not ideal for both compounds, the nucleation step of the growth mechanism is likely to be affected. We are certain that multilayer structures using ALE are possible and that this technique can fabricate high-quality superlattices just as effectively as individual compound layers. However, more work will have to be performed in order to identify and solve the nucleation problem.

4.0 PROGRESS SUMMARY

The technical progress achieved during this program was in the areas of ALE development of zinc chalcogenide materials and application of ALE technology to IR rugate fabrication. In summary we

1. Successfully grew high quality ZnS, ZnSe and ZnTe thin films on (100)-oriented GaAs by thermal evaporation ALE.

2. Conducted exploratory experiments in the area of laser evaporation ALE of zinc chalcogenide materials and found this method to be incompatible with the increased deposition rate requirements for IR rugate fabrication.

3. Had limited success in depositing optical interference device structures by the ALE technique.

5.0 TECHNICAL ISSUES

Some of the most important technical issues facing the use of ALE as a method for fabricating IR rugate filters are growth rate, source material utilization and mechanical reliability of in-vacuum equipment. In order to be a viable technique for fabricating the extremely thick films (> 150 μm) needed for high performance IR rugates, any deposition method must have rates approaching 5-10 Å/s. Because of the large thickness of these filters, source material must be efficiently utilized in order to complete the thick structures without having to break vacuum and replenish source material. In addition, the large number of cycles needed to achieve high performance dictates that many individual layers be deposited if the filter is a "digital" type. This makes mechanical reliability of in-vacuum equipment such as shutters, rotary motion feedthroughs and any moving parts, subject to failure because of the long run times and the large amount of material which must be deposited.

Previous work on the ALE-growth of zinc chalcogenide materials[14] reported exposing the substrates to each element for 7-14 s with an ~ 5 s pause between elements. This algorithm would result in a range of growth rates between 0.12 and 0.075 Å/s; much too slow to be a practical method of depositing thick films. Some important considerations in increasing the growth rate would be; 1) minimizing the source to substrate distance to reduce material transit time, 2) maximizing system pumping speed to reduce the time needed to pump away any excess re-evaporated material; and 3) designing an evaporation system which could produce short, compact bursts of elemental material from the source. These are engineering problems which can be addressed and optimized during the design and construction of the ALE growth chamber. However, the limiting step in the ALE growth of any compound may be the nucleation and growth kinetics at the substrate surface. Because of the equilibrium requirements of this growth technique, any deposition which takes place under nonequilibrium conditions will result in nonuniform or incomplete coverage of the atomic layers. The end result will be loss of thickness control, alteration of stoichiometry and degradation of the film properties. During this program we attempted to optimize the growth parameters to achieve the maximum attainable growth rate. This work resulted in an effective growth rate of between 0.35 and 0.45 Å/s, a significant improvement over the previously reported rates.

An additional requirement for any deposition technique to become a practical means of fabricating IR rugate structures is efficient utilization of source material. In ALE, this is particularly important since only one element is needed at any given moment. Laser evaporation was investigated as a means of conserving source material but S and Zn proved to be incompatible with laser evaporation with 1.06 or 10.6 μm radiation. In order to conserve material while using thermal evaporation, a method to prevent leakage of material while it is not needed must be used. We modified our original thermal source flange by replacing a single rotating shutter, which allowed unneeded material to escape the crucible, with individual shutters over each source. This method proved adequate at minimizing the amount of material lost during crucible dead-time. A more effective source design to reduce material loss and increase beam control would be the use of MBE-type effusion cells which have small needle valves that control the escaping material. The valve portion of these cells are heated so that material does not condense and clog the orifice. In addition the valve seal is sufficient to prevent any leakage of material while the valve is closed.

During thermal evaporation ALE, each shutter must open and close during the deposition of each atomic layer of that element. Because of the large number of atomic layers which make up a rugate structure (e.g., 1.4×10^6 atomic layers in 100 cycles of the design in Fig. 2.6) mechanical reliability of rotary motion feedthroughs and shutters is extremely important. The design of any linkage which connects the shutter to the motor outside of the vacuum should be direct drive, having as few components as possible. This limits the number of possible failure points and simplifies repair and maintenance.

Although laser evaporation did not work with a Nd:YAG laser at powers less than 800 mJ/pulse, this type of evaporation may be feasible at different wavelengths or with a more powerful laser. Because of the large differences in the absorption coefficients of Zn, Te and Se, a variable attenuator would be necessary to limit the power used during the evaporation of the more absorptive elements. However, if the laser power is sufficient to provide a reasonable flux of Zn, then many of the advantages of laser evaporation such as energetic evaporant species and excellent evaporation control could be realized.

6.0 DISCUSSION AND CONCLUSIONS

The objective of this program was to determine the feasibility of using Atomic Layer Epitaxy as a deposition technique for fabricating IR rugate structures. It was known from the outset that ALE, as commonly practiced, possessed the disadvantage of low growth rate, but it was believed that the high-quality epitaxial films and extremely precise thickness control would outweigh this disadvantage. ALE growth of single compound films such as ZnS, ZnSe and ZnTe did produce superior quality epitaxial thin films on GaAs (001)-oriented substrates. However, more work would have to be performed before multilayer structures of any two of these materials could be routinely deposited. The optimum growth conditions established for single compound films do not appear to be applicable to the multilayer structures. The most important consideration appears to be the additional time required for proper nucleation when depositing ZnTe on ZnSe. It is not known at this time why this interface does not equilibrate at the same rate in both directions. If a means of achieving correct nucleation can be found, ALE is capable of producing high-quality epitaxial superlattices of the zinc chalcogenide materials. Even after solving the interface problem, the single most important factor for utilizing the technique will still be growth rate. It appears that the growth kinetics for proper ALE growth will limit the growth rate to ~ 2 Å/s. This rate is simply too slow to be of practical use for fabricating a structure which is in excess of about 10-20 μm in total thickness.

Even with the limited results obtained with ALE under this contract, there are applications for which ALE is extremely attractive. High-quality epitaxial films could be used in guided wave optics where crystalline perfection and bulk-like properties are important. Thin-film devices (< 10 μm) containing II-VI compound semiconductors, in which film quality and film thickness control are essential, are also good candidates for ALE growth. Our conclusions are that, although ALE is capable of producing high-quality epitaxial thin films of ZnS, ZnS and ZnTe, and possibly multilayer structures, it is not practical for use as a technique for fabricating thick IR rugate filters.

7.0 REFERENCES

1. C.H.L. Goodman and M.V. Pessa, J. Appl. Phys. 60, R65 (1986).
2. T. Yao and T. Takeda, Appl. Phys. Lett. 48, 160 (1986).
3. J.G. Nelson, J. Vac. Sci. Tech. A5, 2140 (1987).
4. T. Suntola and J. Antson, U.S. Patent 4058430, 1977.
5. M. Ahonen, M. Pessa and T. Suntola, Thin Sol. Films 65, 301 (1980).
6. M. Pessa and R. Makela, Appl. Phys, Lett. 38, 131 (1981).
7. V.P. Tanninen, M. Oikkonen and T.O. Tuomi, Phys. Stat. Sol. A 67, 573 (1981).
8. M. Pessa, O. Jylha and M.A. Herman, J. Cryst. Growth 67, 255 (1984)
9. M. Pessa, P. Huttunen and M.A. Herman, J. Appl. Phys. 54, 6047 (1983).
10. S.M. Bedair, M.A. Tischler, T. Katsuyama and N.A. El-Masry, Appl. Phys. Lett. 47, 51 (1985).
11. J.I. Nishizawa, H. Abe and T. Kurabayashi, J. Electrochem. Soc. 132, 1197 (1985).
12. J.T. Cheung, Mat. Res. Symp. Proc. 29, 301 (1984).
13. H.H. Li, J. Phys. Chem. Ref. Data 13, 103 (1984).
14. T. Yao, T. Takeda and R. Watanubi, Appl. Phys. Lett. 48, 1615 (1986).

DISTRIBUTION LIST

Number of Copies

1) USA CECOM — 5
CNVEO
AMSEL-RD-NV-L (B.H. Ahn)
Ft. Belvoir, VA 22060-5677

2) DARPA
ATTN: Dr. John Neff — 1
1400 Wilson Blvd
Arlington, VA 22209

3) DARPA — 1
ATTN: Dr. S. Shey
1400 Wilson Blvd
Arlington, VA 22209

4) DARPA — 1
ATTN: Dr. F. Patten
1400 Wilson Blvd
Arlington, VA 22209

5) Commander — 1
USA LABCOM SMO
ATTN: Dr. N. Diakides
2800 Powder Mill Rd
Adelphi, MD 20783

6) Commander — 1
USA AMC Headquarters
ATTN: Mr. R. Vitali
5001 Eisenhower Ave
Alexandria, VA 22333

7) AFWAC/MLPJ — 2
ATTN: Dr. Peter Land
Wright-Patterson AFB, OH 45433

8) Naval Research Laborotary — 1
Code 6607
Mr. Stephen Babjak
4555 Overlook Ave, SW
Washington D.C., 20375

9) Naval Research Laboratory — 1
Code 6557
Dr. Leon Esterowitz
Washington D.C., 20375

10) Commander — 1
US Army Research Office
Box 12211
ATTN: Dr. Robert Lontz
Research Triangle Park, NC 27709

11) US Army Natick Research and Development Center 1
ATTN: Dr. Frank Bisset
Natick, MA 01760-5020

12) Naval Air Development Center 1
ATTN: Dr. Gloria Chisum
Code 60B1
Warminster, PA 18974-5000

13) COMMANDER 1
US Army Research Office
Box 12211
ATTN: Dr. R. Guenther
Research Triangle Park, NC 27709

END

DATE

FILMED

6-1988

DTIC